DIOCOTRON INSTABILITY OF AN INTENSE RELATIVISTIC ELECTRON BEAM IN AN ACCELERATOR

H. C. CHEN
H. S. UHM

NSWC MP 84–346

PLASMA PHYSICS PUBLICATION NO. 84-7

AUGUST 1984

NAVAL SURFACE WEAPONS CENTER
White Oak, Silver Spring, Maryland 20910

Accession Number: 3802

Publication Date: Aug 01, 1984

Title: Diocotron Instability of an Intense Relativistic Electron Beam in an Accelerator

Personal Author: Chen, H.C.; Uhm, H.S.

Corporate Author Or Publisher: Naval Surface Weapons Center, White Oak Laboratory, Silver Spring, MD Report Number: NSWC MP 84-346

Comments on Document: Archive, RRI, DEW

Descriptors, Keywords: Directed Energy Weapon DEW Diocotron Instability Intense Relativistic Electron Beam Accelerator Annular Electron Beam Propagation Electromagnetic Field Physics Kinetics Laser Reaction Perturbation Gro

Pages: 24

Cataloged Date: Oct 19, 1992

Document Type: HC

Number of Copies In Library: 000001

Record ID: 24971

Source of Document: DEW

DIOCOTRON INSTABILITY OF AN INTENSE RELATIVISTIC ELECTRON BEAM IN AN ACCELERATOR

H. C. Chen and H. S. Uhm
Naval Surface Weapons Center
White Oak, Silver Spring, Maryland 20910

Abstract

High current annular electron beam in an accelerator is subject to various instabilities. A general fluid-Maxwell theory of the diocotron instability is developed for an infinitely long and azimuthally symmetric annular electron beam propagating along an external magnetic field. In contrast with the treatment used in the conventional diocotron instability, the assumptions of tenuous electron beam and strong magnetic field have been eliminated. Furthermore, the restriction of infinite axial wavelength perturbation has been removed and the approximation of $\omega \sim ck\beta$ is no longer applied. Instead, we conduct full electromagnetic perturbation in the macroscopic cold fluid description of plasma dynamic with the beam parameters of general interest. In the special case of a sharp boundary density profile, the diocotron instability which dominates in the low frequency region are investigated in a broad range of beam parameters and geometries. The results are significantly different from that obtained from the conventional diocotron instability. The kink mode can be destablizied and the growth rates are much larger for every azimuthal mode.

I. INTRODUCTION

Intense relativistic electron beams have been developed in recent years as a new source of electromagnetic radiation which can be applied to high current electron beam accelerator, collective accelerator, gyrotron and free electron laser, etc. In most particle accelerators,[1] a high-current beam is injected into a low-pressure gas or into an evacuated tube along a strong external magnetic field. The guide magnetic field provides the confinement of the beam which prevents the beam from spreading radially. Otherwise, the instability can be very destructive to the beam. Nevertheless, the regions of stability and instability have been found in some of the experiments and the problem of stability has been considered in most of the theoretical investigations.

Experiments have been going on recently to generate and transport intense relativistic electron beams in gaseous or plasma medium. It has been found that the resistive hose instability is one of the most dangerous perturbations to the propagation beam.[2] However, the stability analyses and plasma particle simulations indicate that the increase of the beam current can reduce the hose growth rate to a large extent. As a result, the beam with high current (> 30 KA) becomes an ultimate choice for the ejection of a relativistic electron beam to the plasma medium. Historically, high current beams have been produced as annular beams guided by a strong magnetic field to reduce beam perpendicular motion. However, it is very often and rather common to have large amplitude beam transverse oscillations observed right after the accelerator. The transverse perturbation can be very destructive to the beam, especially in the region where a rapid magnetic field transition occurs. The

necessity of eliminating this initial perturbation is crucial if stable beam propagation needs to be achieved. In order to have a full understanding of the beam propagation physics, the careful characterization of the beam parameters before ejection to the plasma channel is absolutely essential.

The diocotron instability of a hollow electron beam has been known for a long time since the early crossed field microwave magnetron. For an annular electron beam in the cylindrical geometry, Buneman[3] has considered the diocotron instability in the regime of $\omega_{pb} \sim \omega_c$ while Levy[4] has examined the instability in the case of low beam density and strong magnetic field, i.e., $\omega_{pb} << \omega_c$ where ω_{pb} and ω_c stand for the electron plasma and cyclotron frequency respectively. Since then numerous theoretical work has been done theoretically and most of them consider only perturbations with sufficiently long wavelength ($k \sim 0$). Experimentally, there is some evidence that the lower order diocotron modes have been found in the damaged plate after the target interaction of the annular electron beam. Recently, the filamentation instability ($\ell > 2$) of an annular electron beam along a uniform magnetic field has been studied[5] by using the Vlasov-Maxwell equations. Here, a more complete full electromagnetic treatment of the fluid-Maxwell theory is conducted without any approximations which have been made previously. We want to consider the perturbations not only in the azmuthal ($\ell \neq 0$) but also in the axial directions ($k_z \neq 0$). In addition, the model developed here emphasizes the case for high current electron beam, therefore the assumption of $\omega_{pb} < \omega_c$ is no longer true. Most importantly, the validity of the previous $\omega \sim ck\beta$ assumption in the treatment of the conventional diocotron instability is examined.

A macroscopic cold fluid-Maxwell theory is used to perform the linear stability analysis of an infinitely long intense annular electron beam propagating along an external magnetic field. A brief description of the equilibrium configuration and an outline of the assumptions are given in Section II. In the rigid-rotor and cold laminar flow limit, a dispersion relation is derived in Section III for the general case which results in a general integro-differential equation for the perturbed field. In the special case of a rectangular density profile, a closed algebraic dispersion relation for the complexed eigenfrequency is extracted. The dispersion relation obtained can be used to investigate the instability for a broad range of system parameters. The numerical solutions for the instabilities are presented in Section IV. Finally, the discussion and a few remarks on the finite geometry effect of an accelerator are concluded in Section V.

II. EQUILIBRIUM AND ASSUMPTION

As illustrated in Figure 1, the equilibrium configuration consists of a cylindrically symmetric annular electron beam located between radii R_1 and R_2 in a perfect conducting cylinder of radius R_c. The beam is assumed infinite in the axial direction and aligned parallel to a uniform applied magnetic field. The magnetic field provides the confinement of the annular beam and forbids the spreading in the radial direction. The radial thickness of the annular beam ($R_2 - R_1 = 2a$) is assumed small in comparison with the mean equilibrium radius R_0. As a result, the beam rotation is weakly dependent on r in a slow motion equilibrium which allows us to approximate $\omega_b(r)$ in Eq. (12). The beam under consideration is characterized by the charge q, mass m, axial velocity $c\beta$ and density profile n respectively. It is further assumed that $\nu/\gamma < < 1$ where ν is Budker's parameter. In the cold-fluid model, the flow of electrons can be considered laminar provided that the beam current is much smaller than the Alfven-Lawson space-charge limiting current

$$I < 17000\ \beta\gamma$$

Furthermore, the beam electrons motion are taken to be paraxial so that the axial velocity is very large compared to the transverse velocity and is considered to be a constant i.e., $P_r^2 + P_\theta^2 < < P_z^2$ where $\tilde{P} = (P_r, P_\theta, P_z)$ is the particle momentum. It is noted that the perpendicular motion of beam electron is treated nonrelativistically. We introduce a cylindrical polar coordinate system (r, θ, z) with the z axis coinciding with the axis of symmetry. Analysis of beam dynamic properties is based on a macroscopic cold fluid model. The equation of electron and momentum conservation for the electron fluid can be expressed in the relativistic form as

$$\frac{\partial n}{\partial t} + \nabla \cdot (n \underline{V}) = 0 \tag{1}$$

$$\left(\frac{\partial}{\partial t} + \underline{V} \cdot \nabla\right) \gamma m \underline{V} = q \left(\underline{E} + \underline{V} \times \underline{B}/c\right) \tag{2}$$

where $n(\underline{x},t)$ and $\underline{V}(\underline{x},t)$ are the density and mean velocity of an electron fluid element. $\underline{E}(\underline{x},t)$ and $\underline{B}(\underline{x},t)$ are the electric and magnetic fields respectively. $\gamma = (1 - \beta^2)^{-1/2}$ and $\beta = \frac{V_b}{c}$ are the standard relativistic quantities and c is the speed of light in vacuum. The self-induced electric and magnetic field can be related to the beam density and current by Maxwell's equations. By including the Maxwell equations we have a complete closed system of equations.

In the steady state $(\frac{\partial}{\partial t} = 0)$ the beam is assumed azimuthally symmetric $(\frac{\partial}{\partial \theta} = 0)$ and infinite long and uniform in the axial direction $(\frac{\partial}{\partial z} = 0)$. The equilibrium force balance due to electric and magnetic field in the radial direction gives the angular velocity $\omega_b(r)$ of an electron fluid element in slow rotational equilibrium

$$\omega_{b(r)} = \omega_{pb}^2 \, (1 - R_1^2/r^2)/(2\gamma^2\omega_c) \qquad R_1 < r < R_2 \tag{3}$$

where $\omega_{pb}^2 = 4\pi n \, q^2/\gamma m$ and $\omega_c = qB_0/c\gamma m$ are the electron plasma frequency square and cyclotron frequency respectively, and B_0 is the guided magnetic field. The radial force due to E_r and B_θ is equivalent to an effective radial field $\frac{E_r}{\gamma^2}$ which combined with B_z leads to an azimuthal drift. The effect of positive ions which form an immobile partially neutralizing background is not considered here. It is further assumed that the ion current is equal to zero in the laboratory frame.

III. STABILITY ANALYSIS

We assume, without loss of generality, that all the perturbed quantities have the following wave form in the cylindrical geometry with the sinusoidal time dependence and spatial variation

$$\delta\Phi\ (\underline{x},t) = \delta\Phi(r)\ \exp\left[i(\ell\theta + kz - \omega t)\right] \tag{4}$$

where the oscillating angular frequency ω is assumed to be complex with $\mathrm{Im}(\omega) > 0$, ℓ is the azimuthal harmonic number and k is the propagation wavenumber in the axial direction. We use the linearized fluid-Maxwell equations to investigate the general electromagnetic perturbation for $\ell \geq 1$ and any arbitrary wavenumber k. Let us choose the transverse magnetic (TM) modes such that the magnetic field lies in the cross-sectional plane since all the transverse fields for the TM mode can be expressed in terms of the z-component of the electric field. The determination of the transverse fields therefore can be expressed only in terms of δE_z according to

$$B_t = \left(\frac{\omega^2}{c^2} - k^2\right)^{-1} i\,\frac{\omega}{c}\, e_3 \times \nabla_t E_z \tag{5}$$

$$E_t = \left(\frac{\omega^2}{c^2} - k^2\right)^{-1} \nabla_t(\partial E_z/\partial z) \tag{6}$$

where ∇_t is the transverse two-dimensional gradient operator. From the perturbed Maxwell equation, it is straightforward to express after some algebraic manipulations that the relationship between the perturbed field δE_z and the source terms δn and δJ_z

$$\left(\nabla^2 + \frac{\omega^2}{c^2}\right) \delta E_z = 4\pi i k\left(q\delta n - \frac{\omega}{kc^2}\,\delta J_z\right) \tag{7}$$

δJ_z is the perturbed current in the axial direction such that

$$\delta J_z = q(\delta n V_z + n\,\delta V_z) \tag{8}$$

where δn and δV_z can be obtained by solving a set of first order perturbation equation from Eqs. (1) and (2). With the help of Eqs. (5) and (6), δn and δJ_z can be expressed in terms of δE_z. Therefore, Eq. (7) for δE_z, together with boundary conditions on the field component represented by the scalar function δE_z, specifies a two-point boundary eigenvalue problem which can be solved numerically. For the special case of a square density profile for the hollow beam, the above-mentioned procedure with some straightforward but tedious algebraic manipulations rewrites Eq. (7) in the final form as

$$\begin{aligned}&\left\{\frac{1}{r}\frac{\partial}{\partial r}\left[r(1 + S_1)\frac{\partial}{\partial r}\right] - \frac{\ell^2}{r^2}(1 + S_1) - \left(k^2 - \frac{\omega^2}{c^2}\right)\right\} \delta E_z(r) \\ &= \frac{\ell}{r}\frac{\omega_c}{\Omega}\frac{S_1}{n}\frac{\partial n}{\partial r}\,\delta E_z(r) - \left(k^2 - \frac{\omega^2}{c^2}\right)\left[\frac{\omega_{pb}}{\gamma\Omega_0}\left(1 + \frac{\ell\omega\omega_b}{c^2k^2 - \omega^2}\right)\right]^2 \delta E_z(r)\end{aligned} \tag{9}$$

where the following abbreviations have been used

$$S_1 = \frac{\omega_{pb}^2}{\omega_c^2}\frac{(ck - \omega\beta)^2}{(ck)^2 - \omega^2} \tag{10}$$

$$\Omega = \omega - \ell\omega_b(r) - ck\beta \tag{11}$$

$$\Omega_0 = \omega - \ell\omega_b(R_0) - ck\beta \tag{12}$$

Equation (9) is a second order differential equation for δE_z. Therefore, two boundary conditions namely $\delta E_z(0)$ and $\delta E_z(R_c)$ are needed to specify a two-point boundary eigenvalue problem. The contribution to the first term of the RHS of Eq. (9) becomes two delta functions at the sharp boundaries of the beam. The second term on the other hand is evaluated at R_0 approximately for a thin annular beam. For a given wavenumber k, only certain oscillating frequency ω will be consistent with the differential equation subject to satisfy the boundary condition.

It is noted that the self-induced magnetic field B_θ has been neglected and the condition of slow beam rotation ($\omega_b << \omega_c$) has been used in deriving Eq. (9). We are ready to solve Eq. (9) for the special case of a square density profile hollow beam. Because of the approximation we made in Eq.(12), Eq. (9) becomes the familiar Bessel's equation. The piece-wise solutions for the homogeneous equation of Eq. (9) can be expressed in terms of modified Bessel functions. The eigenfunctions which satisfy Eq. (9) in the three regions can be written down as

$$\delta E_z(r) = \begin{cases} A\, I_\ell(n'r) & 0 < r < R_1 \\ C\, I_\ell(nr) + D\, k_\ell(nr) & R_1 < r < R_2 \\ E\, I_\ell(n'r) + F\, k_\ell(n'r) & R_2 < r < R_c \end{cases} \qquad (13)$$

where A, C, D, E and F are arbitrary constants, and

$$n'^2 = k^2 - \omega^2/c^2$$

$$n^2 = \frac{n'^2}{(1 + S_1)} \left\{1 - \left[\frac{\omega_{pb}}{\gamma\Omega_0}\left(1 + \frac{\ell\omega\omega_b}{c^2k^2 - \omega^2}\right)\right]^2\right\} \tag{14}$$

where n' and n are complex variables. The solutions (13) are required to be continuous and bounded throughout an interval $R_1 < r < R_2$ and to satisfy certain boundary conditions at $r = 0$ and $r = R_c$. In addition, the effect of the delta function can be considered by multiplying both sides of r and integrating over the infinitesimal interval from $r(1 - \varepsilon)$ to $r(1 + \varepsilon)$ with $\varepsilon \to 0$ in the vicinity of $r = R_1$ and R_2 respectively. Applying the jump conditions which yields

$$r(1 + S_1)\frac{\partial}{\partial r}\delta E_z(r)\Bigg|_{R-\varepsilon}^{R+\varepsilon} = \ell S_1 \frac{\omega_c}{\Omega}\delta E_z(r)\Bigg|_R \tag{15}$$

where $R = R_1$ and R_2 for the two sharp boundaries respectively. Therefore, we have obtained 5 linear equations for 5 unknowns A, C, D, E, and F. The dispersion relation is obtained by writing down the condition for the linear homogeneous equations. After some algebraic manipulations, the final result can be expressed as

$$\frac{n'R_1(1 + S_1)\, I'_\ell\,(n'R_1) - I_\ell(n'R_1)A_1}{n'R_1(1 + S_1)\, k'_\ell(n'R_1) - k_\ell(n'R_1)A_1} = \frac{-\, n'R_2(1 + S_1)\, I'_\ell(n'R_2) + I_\ell(n'R_2)A_2}{-\, n'R_2(1 + S_1)\, k'_\ell(n'R_2) + k_\ell(n'R_2)A_2} \tag{16}$$

where I_ℓ, k_ℓ are the modified Bessel function and $I'_\ell(x) \equiv d\, I_\ell(x)/dx$, $k'_\ell(x) \equiv d\, k_\ell(x)/dx$. The following abbreviations have been used

$$A_1 = \ell\, S_1(R_1)\, \omega_c/\Omega + n' R_1\, I'_\ell\,(n'R_1)/I_\ell(n'R_1)$$

$$A_2 = \ell\, S_1(R_2)\, \omega_c/\Omega + \frac{I_\ell(n'R_c)\, k'_\ell(n'R_2) - I'_\ell(n'R_2)\, k_\ell(n'R_c)}{I_\ell(n'R_c)\, k_\ell(n'R_2) - I_\ell(n'R_2)\, k_\ell(n'R_c)} \tag{17}$$

IV. NUMERICAL RESULTS

The general treatment of the electromagnetic perturbation in cylindrical geometry for the diocotron instability has been conducted in Section III using the fluid-Maxwell theory. The dispersion relation of Eq. (16) is solved numerically to determine the growth rate and oscillating frequency of the instability as a function of wavenumber k for a variety of beam parameters.

(a) Non-relativistic case:

For a non-relativistic electron beam (e.g., $\gamma = 1.1$), the growth rate and Doppler-shifted real frequency, both have been normalized to the beam plasma frequency, are plotted versus normalized axial wavenumber in Figures 2a and 2b, respectively. We are interested primarily in the lower azimuthal mode, namely, $\ell = 1$ and a few higher modes. The beam parameters used in Figure 2 are summarized below

$$\gamma = 1.1$$
$$\omega_{pb}R_0/c = .05$$
$$\omega_{pb}/\omega_c = .5$$
$$a/R_0 = .05$$
$$R_0/R_c = .8$$

Note that the Doppler-shifted real frequency ($\omega - ck\beta$) remains very small which characterizes the low frequency diocotron perturbations. It is further noticed that the instability does not occur in the limit of $k \to 0$. In contrast with the conventional diocotron instability, the $\ell = 1$ kink mode can be destabilized for the high current beam case. The instabilities and

associated real Doppler-shifted frequencies as shown in Fig. 2 are almost an even function of wavenumber k except near k = 0. The reason becomes apparent if we examine Eq. (9) carefully. As far as the wavenumber dependence is concerned, the non-symmetric terms with respect to k have been listed in Eqs. (10) thru (12). Nevertheless, because of $\beta \to 0$ for the non-relativistic beam, one can see easily that Eqs. (10), (11) and (12) become symmetric with respect to k especially for larger wavenumber k. However, as wavenumber decreases ($k \to 0$), the non-symmetry property of the instability begins to show in Fig. 2 because Eq. (10) becomes non-symmetry with respect to k again. As comparing to the previous theory, if the approximation of $\omega = ck\beta$ is applied to Eq. (9), then Eq. (9) becomes Eq. (2.6.20) of Davison[7] of the conventional diocotron instability in the electrostatic approximation. Eq. (9) can also be further reduced to Eq. (8) of Reference 8 in the long wavelength perturbation ($k \to 0$) for a tenuous beam in a strong guiding field ($\omega_{pb} << \omega_c$). The growth rates decrease very much when γ increases and the unstable regions shift towards smaller value of k.

(b) Relativistic case:

For the high current electron beam, as the value of $R_0\omega_{pb}/c$ increases, Eq. (9) involving the non-symmetric term with respect to k becomes more important. One can expect the non-symmetric results for the diocotron instability. For the purpose of comparison, we use the same beam geometry as in Figure 2 but change the beam parameter to the following values

$$\gamma = 3$$

$$\omega_{pb}R_0/c = 0.9$$

$$\omega_{pb}/\omega_c = 0.5$$

The results of calculations for the instability are shown in Figure 3. As we expected, the symmetry property of the wave with respect to wavenumber has disappeared. Obviously, Eqs. (10) thru (12) which express the non-symmetrical dependence with respect to k becomes more non-symmetric as $\beta \to 1$ for the relativistic beam case. Unlike the previous results[8,9] of the conventional diocotron instability, the kink mode becomes unstable with relatively large growth rate. As ℓ increases ($\ell > 2$), there are two branches of instability which can be excited. The one with smaller growth rate which exists in both k directions is identified as the conventional diocotron instability. The other branch of the modified diocotron instability has much larger growth rate and can be excited near small k region only. The reason of being might be due to the full electromagnetic treatment of the perturbation for the high current beam. Besides, the approximation $\omega \sim ck\beta$ used in the conventional diocotron instability is no longer applied here. Finally, we we can see in Fig. 3, the new diocotron instabilities for different azimuthal modes occur almost at the same wavenumber (i.e., $ck/\omega_{pb} \sim 0.25$). As we can observe in Eq. (10), there is a singularity for $ck \sim \omega$. That is why the instability can be excited in the positive wavenumber only.

V. CONCLUSIONS

The equilibrium and stability properties of a relativistic nonneutral electron beam have been examined within the framework of the linearized fluid-Maxwell equations. The analysis is carried out for electromagnetic perturbation about an infinitely long annular beam aligned parallel to a uniform magnetic field. One of the most popular cold-fluid instabilities characteristic of a rotating nonneutral hollow beam is the diocotron instability which has been studied previously only in the low-density regime ($\omega_{pe} << \omega_c$). However, it is important to emphasize that the present analysis is not restricted to the low-density regime. The resultant instability for a high current relativistic annular electron beam is somewhat different from the conventional diocotron instability. The most dangerous kink mode ($\ell = 1$) can be destabilized and the growth rates for $\ell \geq 2$ modes are several times larger than the conventional diocotron modes.

The stability analysis of a high-power, high-current electron beam inside an accelerator undoubtly becomes an important subject under investigation, because the instability of the electron beam can cause various kinds of difficulty which will influence the operation for the production and acceleration of an annular beam. The general purpose of this paper is to demonstrate that the high-current annular electron beam can be unstable at parameters of practical interest. Furthermore, from the beam propagation point of view, it is always valuable to understand the initial parameters of the propagating beam. If a beam comes out from an accelerator and suffers initially a large transverse oscillation, then this off-center beam propagating into the magnetic field gradient at transition section to the

plasma would either cause beam expansion or trigger a stronger kink instability. In this case, to produce a high-quality, high-current relativistic electron beam becomes an important issue then the beam propagation. Especially, knowing that the growth rate for the diocotron mode increases as the current increases.

Finally, if we examine Figure 3b carefuly, we can estimate the group velocity which approaches the beam velocity for the maximum growth rate of the diocotron mode, i.e. $\frac{\partial \omega}{\partial k} = V_g \simeq \beta c$. In other words, the instability follows closely with the beam head where the maximum growth occurs for the perturbation. It is vital to the beam head and therefore crucial to the operation of the high-current accelerator. However, the beam we considered here has been assumed to be infinitely long. In the real application, when the diocotron mode with axial wavelength larger than the drifting tube of the accelerator, the theory derived here may not be necessarily still valid and the important effect of finite geometry on the diocotron instability has to be taken into account. Further studies similar to the treatment in Reference 10 should be considered for this type of problem.

ACKNOWLEDGEMENTS

This research was supported by the Independent Research Fund at the Naval Surface Weapons Center.

REFERENCES

1. T. R. Lockner and M. Friedman, IEEE Trans. Nucl. Sci. 26, 4238 (1979).
   T. R. Lockner and M. Friedman, J. Appl. Phys. 51, 6068 (1981).

2. H. S. Uhm and M. Lampe, Phys. Fluids 23, 1574 (1980).
   W. M. Sharp, M. Lampe and H. S. Uhm, Phys. Fluids 25, 1456 (1982).

3. O. Buneman, J. Electron 3, 1 (1957).

4. R. H. Levy, Phys. Fluids 8, 1288 (1965).

5. J. G. Siambis and H. S. Uhm, Phys. Fluids, 25, 566, 1982.

6. J. D. Lawson, The Physics of Charged-Particle Beams, (Clarendon Press, Oxford, 1977).

7. R. C. Davidson, Theory of Non-Neutral Plasmas,(Benjamin, New York, 1974).

8. H. C. Chen and P. J. Palmadesso, Phys. Fluids 24, 357 (1981).

9. H. S. Uhm and J. G. Siambis, Phys. Fluids 22, 2377 (1979).

10. S. A. Prasad and T. M. O'Neil, Phys. Fluids 26, 665 (1983).

FIGURE CAPTIONS

Figure 1. Longitudinal and cross section of equilibrium configuration and coordinate system

Figure 2a. The diocotron growth rate versus wavenumber for different azimuthal number. The beam parameters are $\gamma = 1.1$, $a/R_0 = .05$, $\omega_{pb} R_0/c = .05$, $\omega_{pb}/\omega_c = .5$ and $R_0/R_c = .8$.

Figure 2b. The real Doppler-shift real frequency of the diocotron instability corresponds to Figure 2a.

Figure 3a. The diocotron growth rate versus wavenumber for different azimuthal number. The beam parameters are $\gamma = 3$, $a/R_0 = .05$, $\omega_{pb}R_0/c = .5$, $\omega_{pb}/\omega_c = .5$ and $R_0/R_c = .8$.

Figure 3b. The real Doppler-shift real frequency of the diocotron instability corresponds to Figure 3a.

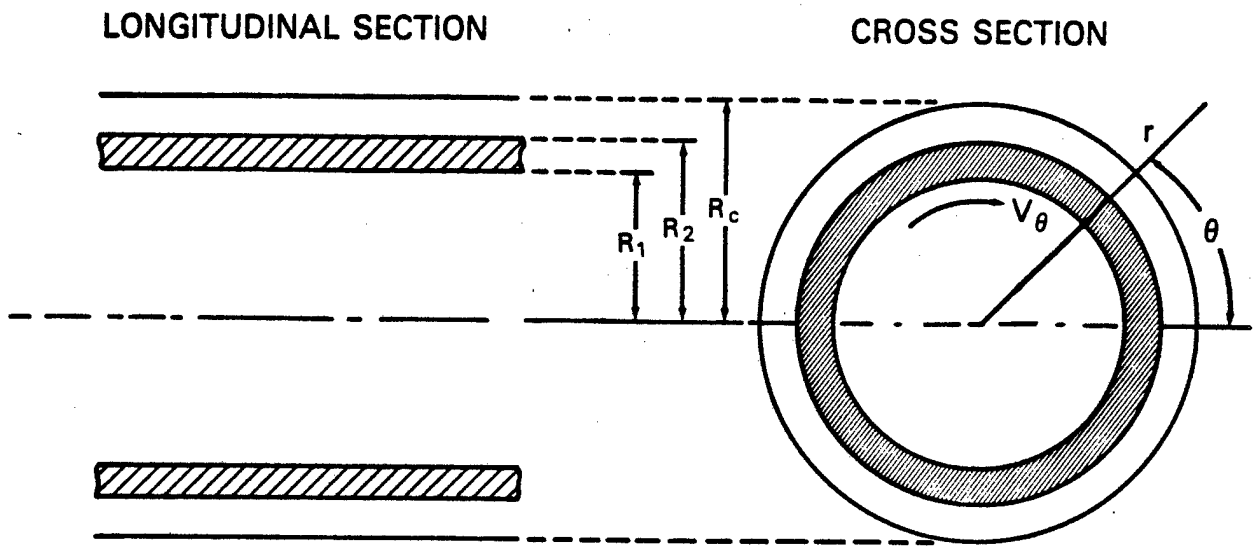

Figure 1

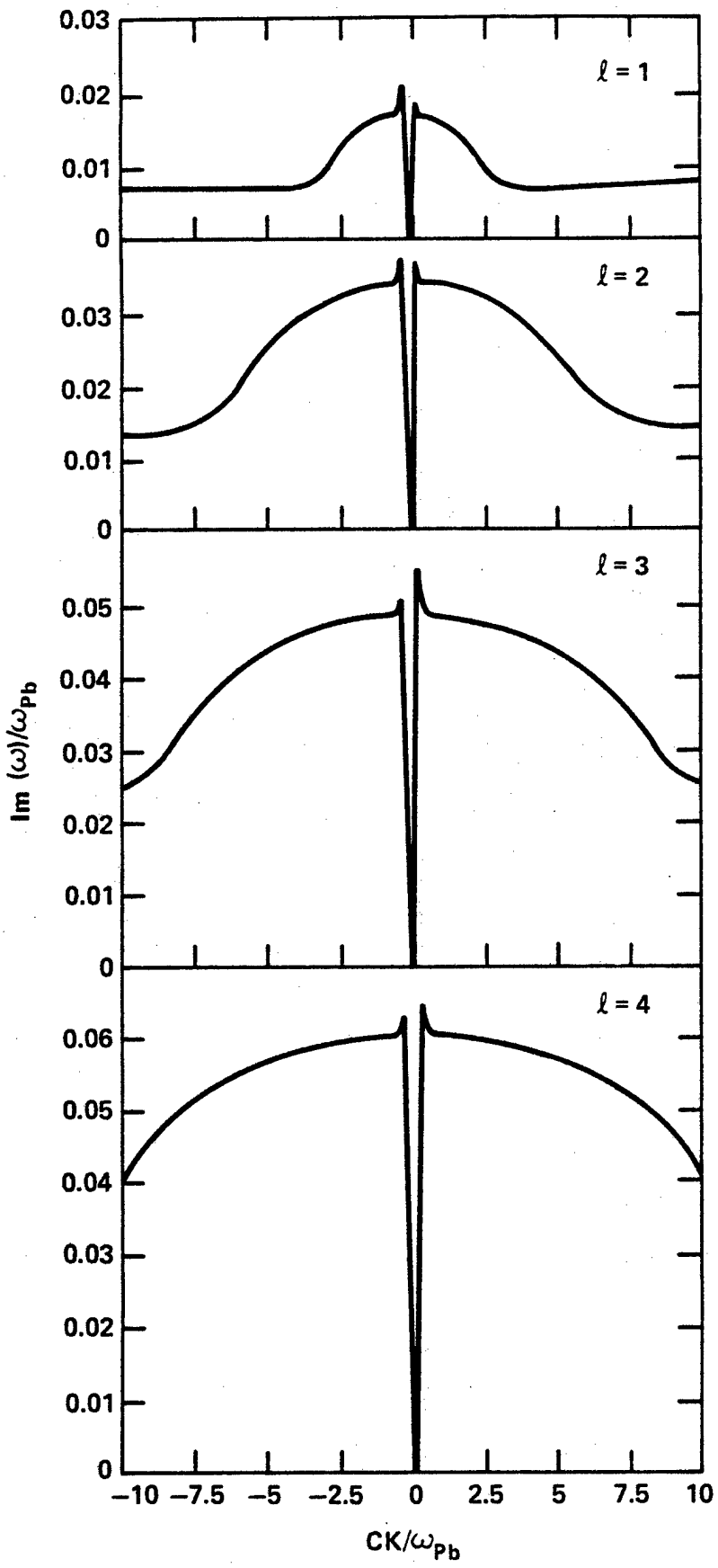
0.03
0.02
0.01
0
ℓ = 1
ℓ = 2
0.03
0.02
0.01
0
ℓ = 3
0.05
0.04
0.03
0.02
0.01
0
ℓ = 4
0.06
0.05
0.04
0.03
0.02
0.01
0
Im (ω)/ω_Pb
−10 −7.5 −5 −2.5 0 2.5 5 7.5 10
CK/ω_Pb

Figure 2a

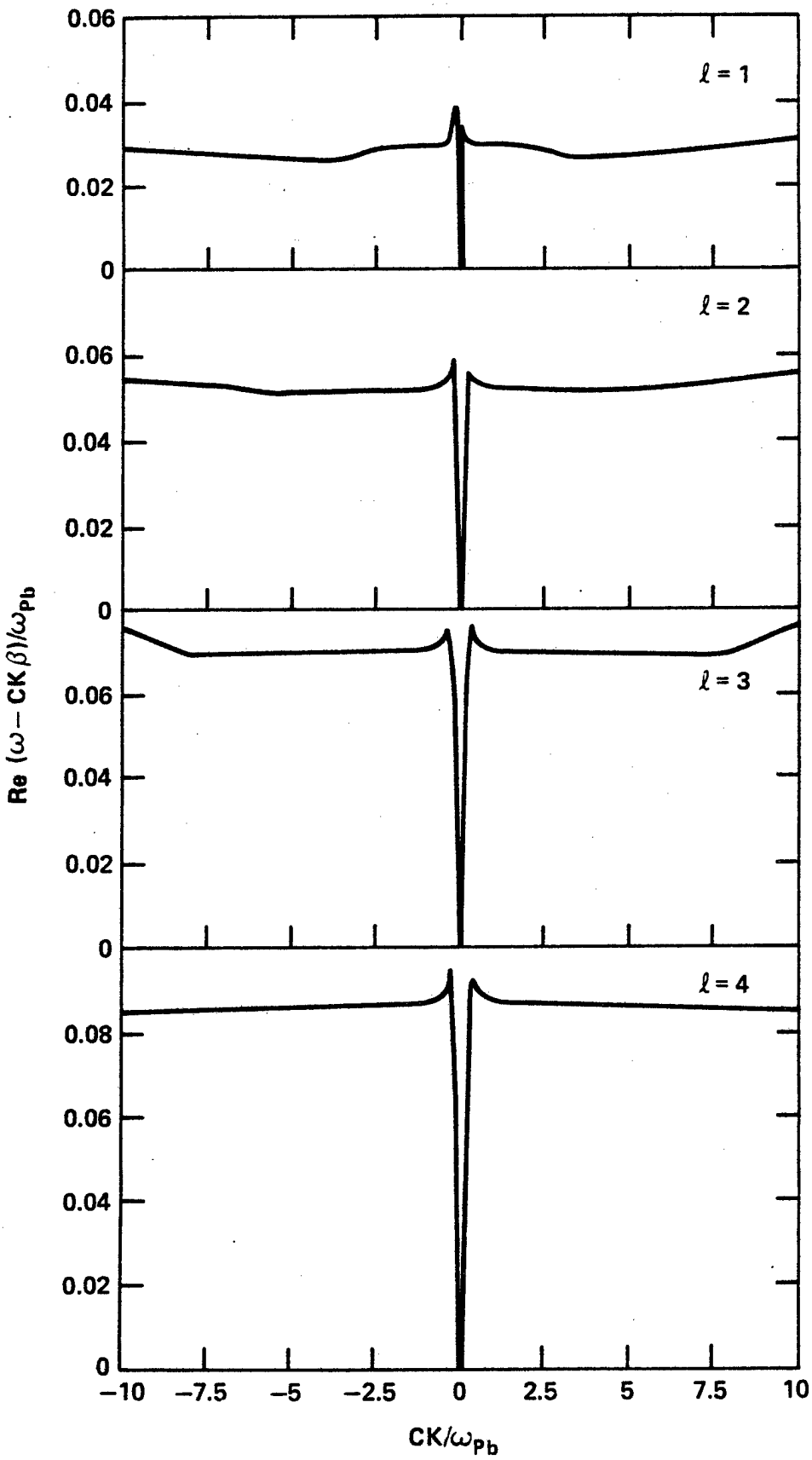
0.06
0.04
0.02
0
ℓ = 1
ℓ = 2
ℓ = 3
ℓ = 4
0.08
Re (ω − CKβ)/ωPb
−10
−7.5
−5
−2.5
0
2.5
5
7.5
10
CK/ωPb

Figure 2b

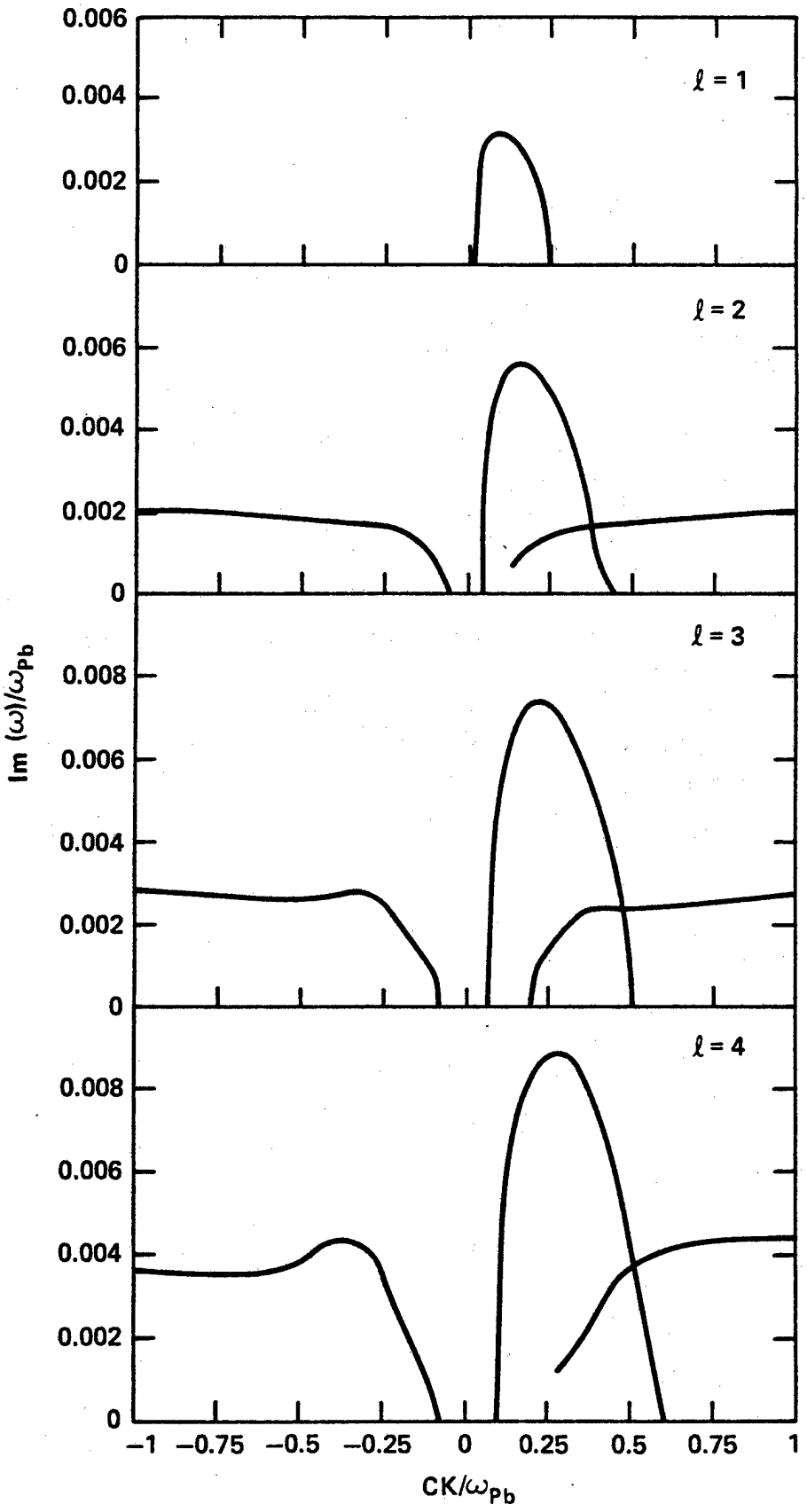
0.006
0.004
0.002
0
ℓ = 1
ℓ = 2
0.008
ℓ = 3
ℓ = 4
Im (ω)/ω_Pb
−1
−0.75
−0.5
−0.25
0
0.25
0.5
0.75
1
CK/ω_Pb

Figure 3a

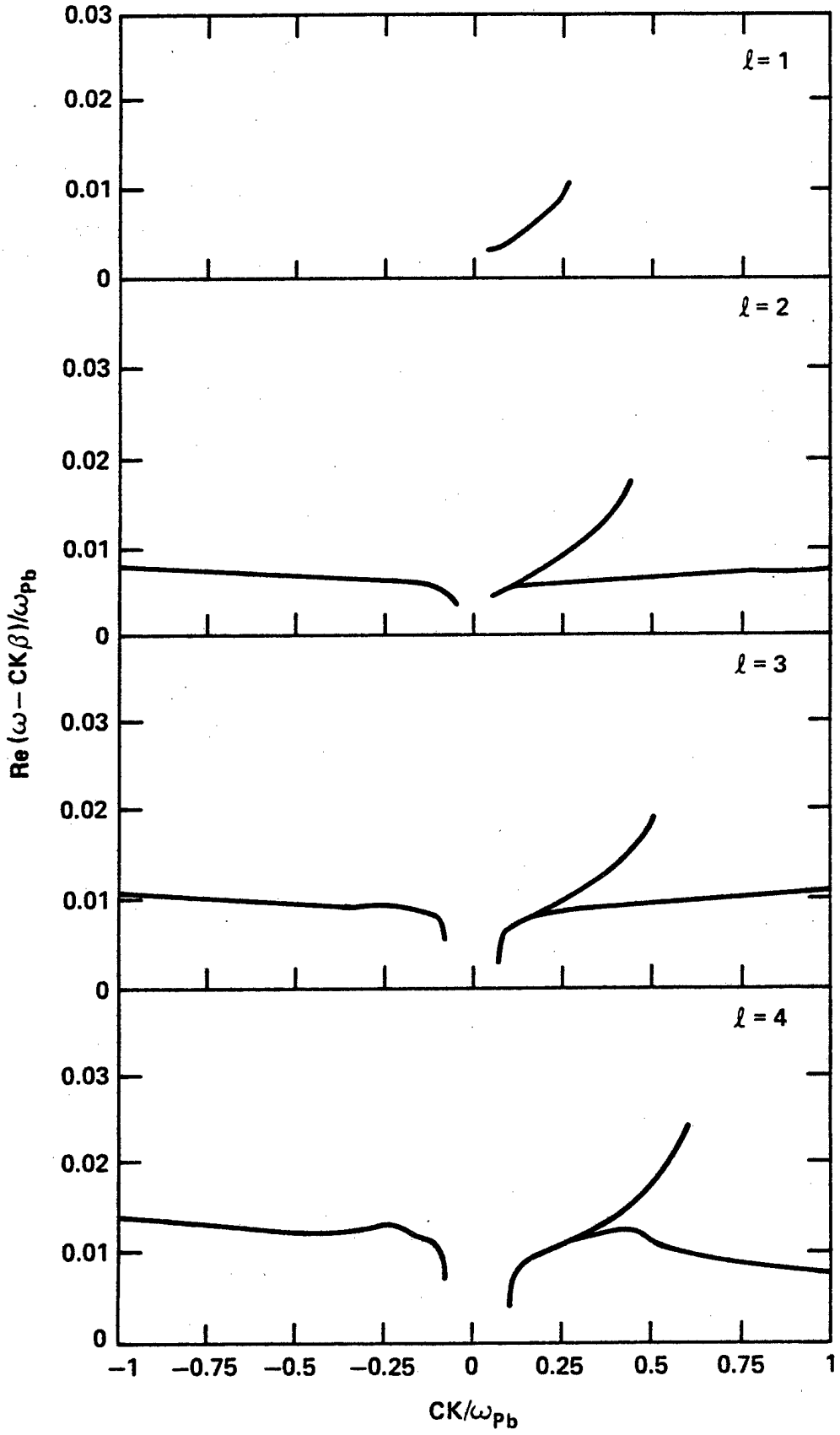
0.03
0.02
0.01
0
ℓ = 1
ℓ = 2
ℓ = 3
ℓ = 4
Re (ω − CKβ)/ωPb
−1
−0.75
−0.5
−0.25
0
0.25
0.5
0.75
1
CK/ωPb

Figure 3b